Inorganic Chemistry

pubs.acs.org/IC

Communication

Synthesis and Spectroscopic Investigation of a Hexaaza Lanthanum(III) Macrocycle with a Hybrid-Type G4 DNA Stabilizing Effect

Marta A. Fik-Jaskółka,* Izabela Pospieszna-Markiewicz, Giovanni N. Roviello, Maciej Kubicki, Wanda Radecka-Paryzek, and Violetta Patroniak*

Cite This: *Inorg. Chem.* 2021, 60, 2122–2126

Read Online

ACCESS | Metrics & More | Article Recommendations | Supporting Information

ABSTRACT: Herein we present a mononuclear lanthanum(III) complex obtained in a template cyclocondensation reaction of lanthanum(III) nitrate salt, 1,2-propanediamine, and 2,6-diacetylpyridine (**LaPA** complex). A preliminary investigation of the biological potential of this compound was conducted using a biomedically relevant target Tel26. We found that, different from parallel G4, antiparallel G4, and duplex DNA, only a hybrid-type G4 structure of Tel26 in a K^+ solution was significantly stabilized by ≥7 °C, which emerged in our UV melting studies. Moreover, **LaPA** induced structural changes in the Tel26 structure in a K^+-deprived solution, suggesting that it may also lead to conformational changes in "non-G4" telomeric DNA.

The G-quadruplex (G4) is a noncanonical DNA structure formed in the guanine-rich regions and preserved by Hoogsteen interactions.[1] Only in 2013 were G4s shown to exist in human genome by visualization using a immunofluorescence staining method with a specific BG4 antibody.[2] They are mostly present in the key regulatory regions of the human genome such as promoters and gene bodies.[3] Moreover, they were revealed to form at the ends of the chromosomes in the regions called telomeres. Hence, they are expected to be involved in maintaining the chromosome stability by preventing the accidental damage of genetic material.[4]

Telomeric DNA, when structured in the G4 form, cannot be recognized by telomerase. This inhibits the telomere lengthening, notably responsible for cancer cell immortality. Thus, directing ligands to stabilize specific telomeric G4-structured DNA constitutes a valuable anticancer strategy.[5] We have recently reported on the telomeric DNA binding capacity of phenylalanine, as verified with Tel26 and Pu22.[6]

Several examples of G4 targeting derivatives are based on planar organic heteroaromatic systems and are able to interact through $\pi-\pi$-stacking, hydrogen-bonding, and electrostatic interactions at the apex and with the loops of G4s, as well as intercalate between G quartets.[7] So far, mostly derivatives of pyridine, acridine, porphyrin, phenanthrene, and naphthalene-diimide are known as G4 DNA targeting agents and stabilizers.[8] However, there are also some reports on macrocyclic entities such as hexaoxazoles, which are able to selectively induce the antiparallel G4 DNA structure of Tel24.[9] The studies available on this topic also show that metal complexes can play an important role as G4 DNA binders.[10] Although the actual function of G4 DNA folds is still under investigation, their relevance is widely recognized, justifying the current interest in the development of new molecules able to stabilize the G4 structures of interest.[11]

An encouraging pathway to build the macrocyclic planar complexes of interest arises from the core concept of supramolecular chemistry: self-assembly. A properly designed macrocycle can be formed in a one-pot synthesis in high yields.[12] The molecular ring size and metal−ligand interactions are relevant in the context of application as biomolecule targeting systems. Therefore, flat macrocycles are able to selectively interact with specific structures of nucleic acids.[13]

In the present work, we report a mononuclear lanthanum(III) complex with an 18-membered hexaaza macrocyclic ligand. The described compound acts as a parallel/antiparallel hybrid-type G4 DNA stabilizer, while it destabilized parallel G4 and duplex DNA and had no influence on the antiparallel DNA stability, as shown by UV melting studies. Additionally, circular dichroism (CD), UV, fluorescence, and scanning electron microscopy (SEM) studies were performed to better elucidate the observed phenomena.

Herein, we report on the formation of a mononuclear lanthanum(III) nitrate complex of a hexaaza macrocyclic ligand of the formula $[La(C_{24}H_{30}N_6)(NO_3)_2CH_3OH]NO_3$, which is soluble and stable in water (Figure S1). A template reaction of lanthanum(III) nitrate salt, 1,2-propanediamine, and 2,6-diacetylpyridine allows one to obtain the **LaPA** complex of an 18-membered macrocyclic ligand as a result of [2 + 2] cyclocondensation (Scheme 1). The compound was characterized by electrospray ionization mass spectrometry

Received: November 3, 2020
Published: February 2, 2021

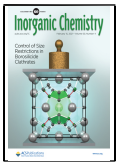

https://dx.doi.org/10.1021/acs.inorgchem.0c03260
Inorg. Chem. 2021, 60, 2122–2126

(Figure S2), IR (Figure S3), and elemental analysis (see the Supporting Information).

Scheme 1. Template Synthesis of the LaPA Macrocycle

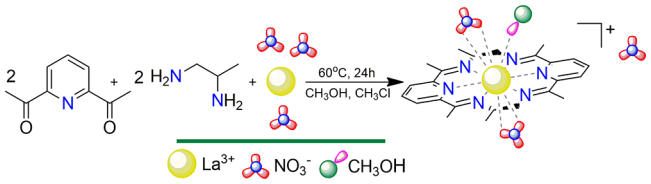

As revealed by X-ray diffraction measurement (Figures 1 and S4 and Table S1), the coordination sphere of lanthanum(III) is

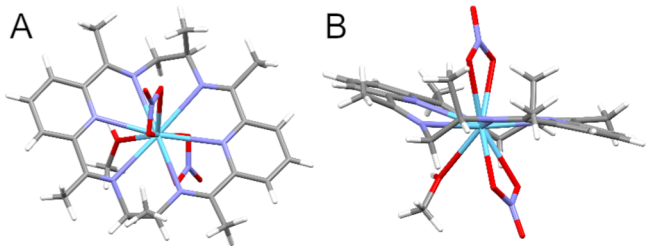

Figure 1. Perspective view of the macrocycle **LaPA** in the top-to-bottom (A) and side (B) views.

filled by six nitrogen atoms (four nitrogen atoms from azomethine groups and two nitrogen atoms from pyridines) and five oxygen atoms (four oxygen atoms from two nitrate groups behaving as bidentate chelators and one oxygen atom from a methanol molecule). Hence, the coordination number of lanthanum(III) is formally equal to 11. A similar coordination was previously observed in a number of lanthanide complexes with hexaaza macrocycles.[14] It might be noted that such a large coordination number is relatively rare. In the Cambridge Structural Database,[15] there are 14063 structures of lanthanide complexes with coordination number 9, while only 514 have coordination number 11 or higher. Among those 514 complexes, 346 have NO_3^- ligands (in the chelating disposition). The close vicinity of available oxygen atoms seems to prefer the high coordination numbers: 67.3% of all complexes compared with 16.4% for coordination number 9. The macrocycle, with a roughly planar skeleton, is close to mirror C_s symmetry (cf. torsion angles). Its planarity and the presence of the central cavity filled with positively charged lanthanum(III) became the foundation for the evaluation of **LaPA** as a G4 DNA binder. The macrocycle is 12.77 Å long and 9.76 Å wide, and the thickness between the two most distant oxygen atoms from nitrates is 8.52 Å. In the G4 DNA hybrid-1 structure,[16] the minor and major grooves are 6.16 and 9.62 Å wide, respectively, and the distance between the stacked tetrads is ca. 3.18 Å. Because of this size mismatch, it is envisaged that the binding and assembly of the **LaPA**–Tel26 complex could occur at the apex of the stacked tetrads through multiple interactions (π–π-stacking, hydrogen-bonding, and electrostatic interactions) stabilizing the loop and flanking regions.[10b]

In order to explore the potential of **LaPA** to interact with G4 DNA structures, we have selected three G-rich strands of DNA forming various G4 structures: Pu22 forming parallel G4,[17] Tel22 forming antiparallel G4 in the presence of Na^+,[18] and Tel26 folding into a hybrid-type parallel–antiparallel G4[19] in K^+ solutions. Our main goal was to obtain a macrocycle that selectively targets the G4s; therefore, the duplex DNA was also tested because binding to it would be clearly undesired as it could diminish the potential therapeutic effects of a candidate as a G4 DNA binder. In this study, the buffers were chosen so as to obtain distinct G4s that are not too stable for the binding experiments (Table S2). Because the experimental conditions are quite different for each oligonucleotide, one has to be aware that no quantitative comparison between various DNA strands can be made here.

In an initial UV-based thermal stabilization screening, we noticed that **LaPA** provokes a ~2–4 °C structural destabilization of both duplex and parallel G4 (Pu22) DNA, while it causes no significant effect on antiparallel DNA, as verified using Tel22 in a Na^+ solution (Figure S5 and Table 1).

Table 1. ΔT_m (°C) for Complexes of LaPA with Duplex DNA, Pu22, Tel22, and Tel26 (First Derivatives Shown in Figures S9–S12)[a]

sample	1 equiv of **LaPA**	2 equiv of **LaPA**
duplex DNA	−1.9 ± 0.4	−3.6 ± 0.4
Pu22	−1.6 ± 0.4	−3.6 ± 0.6
Tel22	+0.3 ± 0.4	−0.4 ± 0.4
Tel26	+7.9 ± 0.4	+6.4 ± 0.6

[a]The results are reported as mean ± standard deviation values. 1 equiv = 2.5 μM.

Conversely, in the case of the hybrid-type parallel–antiparallel G4 structure of Tel26 in a K^+ solution, **LaPA** led to a ~7 °C stabilization effect (Figure 2A and Table 1), a feature that attracted our interest because of the above-mentioned potential of Tel26 stabilizers.[20]

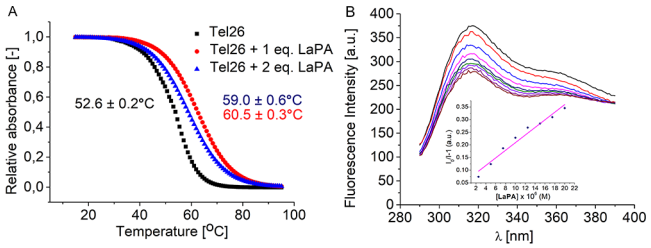

Figure 2. UV melting curves of Tel26 alone and with **LaPA** (A) and fluorescence quenching of Tel26 with the incremental addition (1–8 equiv) of **LaPA** (B). Stern–Volmer plot $I_0/I - 1$ versus [**LaPA**] at the fixed wavelength λ = 312 nm: ●, experimental data points; solid line, linear fitting of the data (inset in part B). Buffer: 10 mM Tris, 100 mM KCl, pH = 7.4. 1 equiv = 2.5 μM.

Moreover, the fluorescence titration experiments performed on different oligonucleotides showed that **LaPA** quenches the intrinsic emission[21] of Tel26 (Figure 2B). Conversely, it has a negligible impact on the intrinsic emission of other oligonucleotides (Figure S6). The observed hypochromicity without any significant shift in the emission spectrum of Tel26 suggests that the macrocycle, in fact, may directly interact with the terminal G-tetrads, which found confirmation in the CD intensity increase in the spectrum of **LaPA**–Tel26 complex (Figure S7A). Furthermore, to obtain more quantitative information, the quenching constant K_{SV} was calculated from the Stern–Volmer equation (see the Supporting Information)[22] and is equal to 1.5 × 10^4 M^{-1} (Figure 2B, inset).

https://dx.doi.org/10.1021/acs.inorgchem.0c03260
Inorg. Chem. 2021, 60, 2122–2126

Knowing that the fluorescence lifetime τ of biomolecules is $\sim 10^{-8}$ s, the quenching rate constant k_q of Tel26 was determined from the equation $K_{SV} = k_q\tau_0$[23] as 1.5×10^{12} $M^{-1}\cdot s^{-1}$. Similar values were obtained in the case of allocryptopine ($K_{SV} = 1.0 \times 10^5$ M^{-1}; $k_q = 4.2 \times 10^{13}$ $M^{-1}\cdot s^{-1}$), which binds partially in the loops and through end stacking to the hybrid-type G4. Higher values of K_{SV} and k_q would suggest that groove binding of the compounds may occur.[24]

It needs to be noted that UV titration and CD studies of Pu22 and Tel22 with **LaPA** do not reveal any significant structural changes in the spectra of oligonucleotides (Figures S7B,C and S8).[25]

The CD spectrum of the folded hybrid-type parallel–antiparallel telomeric G4 is characterized by a negative band at 240 nm, and the two positive bands at ca. 265 and 290 nm (Figure S7A),[26] while a parallel Pu22 G4 lacks the long-wavelength band (Figure S7B). An antiparallel telomeric G4 exhibits one negative band at 265 nm and two positive bands at 245 and 295 nm (Figure S7C).[26] In a K^+-deprived solution, we obtained a CD spectrum for Tel26 exhibiting two strong bands—a negative band at 240 nm and a positive band at 260 nm—and a bump at ca. 292 nm, which was previously associated with the "non-G4" form of this G-rich DNA[5c] (Figure 3A). Upon ligand addition, CD spectral bands

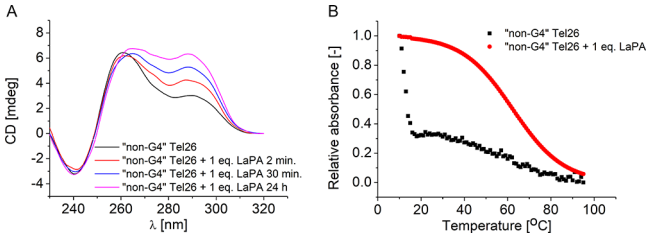

Figure 3. "Non-G4" Tel26 in the absence of K^+ and with **LaPA**: CD studies (A) and UV–vis melting experiments (B; the first derivative is shown in Figure S13). 1 equiv = 2.5 μM.

underwent significant changes, as reported in Figure 3A, clearly indicating that **LaPA** causes conformational changes in the "non-G4" Tel26.[27] Interestingly, when the "non-G4" Tel26 was annealed in the presence of **LaPA**, a melting sigmoid with a high T_m of 62.0 ± 0.6 °C in the UV melting experiment was observed, testifying to the formation of a "non-G4" Tel26–**LaPA** stable complex (Figure 3B).

In order to better characterize the complex formation occurring between "non-G4" Tel26 and **LaPA**, we performed also a SEM analysis of the morphologies adopted by the "non-G4" Tel26–**LaPA** complex. SEM images of this complex shown in the micrographs (Figure 4) revealed spherical particles of width ranging from 3 μm up to 8 μm able to further agglomerate. It is analogous to other literature reports on nucleic acid complexes, which induce the clustering of several nanofibers into larger aggregates (Figure 4B).[6a,28]

Herein, we described the synthesis and characterization of the lanthanum(III) complex $[La(C_{24}H_{30}N_6)(NO_3)_2(CH_3OH)]NO_3$, indicated as **LaPA**, whose potential in biomedicine was explored by our preliminary studies. We used UV, CD, and fluorescence spectroscopies to investigate the ability of **LaPA** to interact with different DNA models, including duplex DNA and oligonucleotides, forming various G4 structures: parallel Pu22, antiparallel Tel22, and hybrid-

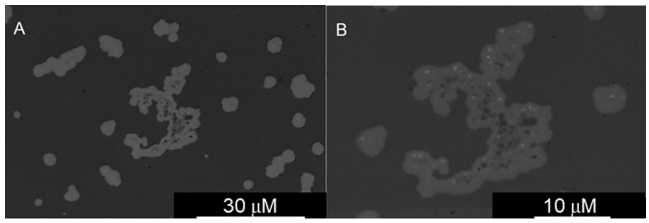

Figure 4. SEM micrographs of Tel26 at concentration 2.5 μM folded in the presence of 1 equiv of **LaPA** in a Tris buffer (10 mM Tris, pH = 7.4).

type parallel–antiparallel Tel26. We found that **LaPA** was able to stabilize hybrid-type G4 but not parallel and antiparallel G4 or double-helical DNA. The **LaPA**–Tel26 complex was endowed with good stability ($T_m \geq 60$ °C), even in the absence of K^+, suggesting that the lanthanum(III) derivative is intrinsically able to form complexes with "non-G4" Tel26. A tendency of Tel26 to form spherical entities in the presence of a **LaPA** binder was also evidenced by SEM. We hypothesize that **LaPA** is an active agent binding probably by π–π-stacking and electrostatic interactions to the apex of the folded hybrid-type G4 DNA, thus stabilizing it.

■ ASSOCIATED CONTENT

Supporting Information

The Supporting Information is available free of charge at https://pubs.acs.org/doi/10.1021/acs.inorgchem.0c03260.

Materials and physical measurements, stability of LaPA, synthesis, X-ray crystallography, oligonucleaoties and preparation of samples, UV–vis studies, CD, intrinsic fluorescence measurements, SEM, results of DNA binding studies, and G4 structure induction of Tel26 (PDF)

Accession Codes

CCDC 2031368 contains the supplementary crystallographic data for this paper. These data can be obtained free of charge via www.ccdc.cam.ac.uk/data_request/cif, or by emailing data_request@ccdc.cam.ac.uk, or by contacting The Cambridge Crystallographic Data Centre, 12 Union Road, Cambridge CB2 1EZ, UK; fax: +44 1223 336033.

■ AUTHOR INFORMATION

Corresponding Authors

Marta A. Fik-Jaskółka – *Faculty of Chemistry and Centre for Advanced Technology, Adam Mickiewicz University in Poznań, 61-614 Poznań, Poland;* orcid.org/0000-0002-4963-5803; Email: martafik@amu.edu.pl

Violetta Patroniak – *Faculty of Chemistry, Adam Mickiewicz University in Poznań, 61-614 Poznań, Poland;* Email: violapat@amu.edu.pl

Authors

Izabela Pospieszna-Markiewicz – *Faculty of Chemistry, Adam Mickiewicz University in Poznań, 61-614 Poznań, Poland*

Giovanni N. Roviello – *Institute of Biostructures and Bioimaging, National Research Council, 80134 Napoli, Italy;* orcid.org/0000-0002-6978-542X

Maciej Kubicki – *Faculty of Chemistry, Adam Mickiewicz University in Poznań, 61-614 Poznań, Poland;* orcid.org/0000-0001-7202-9169

https://dx.doi.org/10.1021/acs.inorgchem.0c03260
Inorg. Chem. 2021, 60, 2122–2126

Wanda Radecka-Paryzek − *Faculty of Chemistry, Adam Mickiewicz University in Poznań, 61-614 Poznań, Poland*

Complete contact information is available at: https://pubs.acs.org/10.1021/acs.inorgchem.0c03260

Author Contributions

The manuscript was written through contributions of all authors. All authors have given approval to the final version of the manuscript.

Funding

The work was supported by the National Science Centre in Poland in the framework of SONATINA Grant 2017/24/C/ST5/00181.

Notes

The authors declare no competing financial interest.

■ ACKNOWLEDGMENTS

Dedicated to Professor Bogdan Marciniec on the occasion of 80th birthday. Prof. Artur Stefankiewicz is gratefully acknowledged for help with the JASCO V-750 spectrophotometer. We thank Dr. Mirosława Skupińska for help in understanding the LaPA−G4 interactions and Dominika Klimek for help with LaPA crystallization.

■ REFERENCES

(1) Henderson, E.; Hardin, C. C.; Walk, S. K.; Tinoco, I.; Blackburn, E. H. Telomeric DNA oligonucleotides form novel intramolecular structures containing guanine·guanine base pairs. *Cell* **1987**, *51* (6), 899−908.

(2) Biffi, G.; Tannahill, D.; McCafferty, J.; Balasubramanian, S. Quantitative visualization of DNA G-quadruplex structures in human cells. *Nat. Chem.* **2013**, *5* (3), 182−186.

(3) Huppert, J. L.; Balasubramanian, S. Prevalence of quadruplexes in the human genome. *Nucleic Acids Res.* **2005**, *33* (9), 2908−2916.

(4) (a) Müller, S.; Kumari, S.; Rodriguez, R.; Balasubramanian, S. Small-molecule-mediated G-quadruplex isolation from human cells. *Nat. Chem.* **2010**, *2* (12), 1095−1098. (b) Pirota, V.; Stasi, M.; Benassi, A.; Doria, F. An overview of quadruplex ligands: Their common features and chemotype diversity. In *Annual Report on Medicinal Chemistry*; Neidle, S., Ed.; Academic Press, 2020; Vol. *54*, Chapter 6, pp 163−196.

(5) (a) Zhou, G.; Liu, X.; Li, Y.; Xu, S.; Ma, C.; Wu, X.; Cheng, Y.; Yu, Z.; Zhao, G.; Chen, Y. Telomere targeting with a novel G-quadruplex-interactive ligand BRACO-19 induces T-loop disassembly and telomerase displacement in human glioblastoma cells. *Oncotarget* **2016**, *7* (12), 14925−14939. (b) Carella, A.; Roviello, V.; Iannitti, R.; Palumbo, R.; La Manna, S.; Marasco, D.; Trifuoggi, M.; Diana, R.; Roviello, G. N. Evaluating the biological properties of synthetic 4-nitrophenyl functionalized benzofuran derivatives with telomeric DNA binding and antiproliferative activities. *Int. J. Biol. Macromol.* **2019**, *121*, 77−88. (c) Musumeci, D.; Mokhir, A.; Roviello, G. N. Synthesis and nucleic acid binding evaluation of a thyminyl l-diaminobutanoic acid-based nucleopeptide. *Bioorg. Chem.* **2020**, *100*, 103862−103870.

(6) (a) Fik-Jaskółka, M. A.; Mkrtchyan, A. F.; Saghyan, A. S.; Palumbo, R.; Belter, A.; Hayriyan, L. A.; Simonyan, H.; Roviello, V.; Roviello, G. N. Spectroscopic and SEM evidences for G4-DNA binding by a synthetic alkyne-containing amino acid with anticancer activity. *Spectrochim. Acta, Part A* **2020**, *229*, 117884−117884. (b) Fik-Jaskółka, M. A.; Mkrtchyan, A. F.; Saghyan, A. S.; Palumbo, R.; Belter, A.; Hayriyan, L. A.; Simonyan, H.; Roviello, V.; Roviello, G. N. Biological macromolecule binding and anticancer activity of synthetic alkyne-containing l-phenylalanine derivatives. *Amino Acids* **2020**, *52* (5), 755−769.

(7) (a) Ma, Y.; Iida, K.; Sasaki, S.; Hirokawa, T.; Heddi, B.; Phan, A. T.; Nagasawa, K. Synthesis and Telomeric G-Quadruplex-Stabilizing Ability of Macrocyclic Hexaoxazoles Bearing Three Side Chains. *Molecules* **2019**, *24*, 263. (b) Suto, R. K.; Edayathumangalam, R. S.; White, C. L.; Melander, C.; Gottesfeld, J. M.; Dervan, P. B.; Luger, K. Crystal Structures of Nucleosome Core Particles in Complex with Minor Groove DNA-binding Ligands. *J. Mol. Biol.* **2003**, *326* (2), 371−380. (c) Kaushik, M.; Kaushik, S.; Roy, K.; Singh, A.; Mahendru, S.; Kumar, M.; Chaudhary, S.; Ahmed, S.; Kukreti, S. A bouquet of DNA structures: Emerging diversity. *Biochem. Biophys. Rep.* **2016**, *5*, 388−395.

(8) (a) Asamitsu, S.; Bando, T.; Sugiyama, H. Ligand Design to Acquire Specificity to Intended G-Quadruplex Structures. *Chem. - Eur. J.* **2019**, *25* (2), 417−430. (b) Recagni, M.; Greco, M. L.; Milelli, A.; Minarini, A.; Zaffaroni, N.; Folini, M.; Sissi, C. Distinct biological responses of metastatic castration resistant prostate cancer cells upon exposure to G-quadruplex interacting naphthalenediimide derivatives. *Eur. J. Med. Chem.* **2019**, *177*, 401−413. (c) Liu, L.-Y.; Liu, W.; Wang, K.-N.; Zhu, B.-C.; Xia, X.-Y.; Ji, L.-N.; Mao, Z.-W. Quantitative Detection of G-Quadruplex DNA in Live Cells Based on Photon Counts and Complex Structure Discrimination. *Angew. Chem., Int. Ed.* **2020**, *59* (24), 9719−9726.

(9) Tera, M.; Ishizuka, H.; Takagi, M.; Suganuma, M.; Shin-Ya, K.; Nagasawa, K. Macrocyclic hexaoxazoles as sequence-and mode-selective G-quadruplex binders. *Angew. Chem., Int. Ed.* **2008**, *47* (30), 5557−5560.

(10) (a) Georgiades, S. N.; Abd Karim, N. H.; Suntharalingam, K.; Vilar, R. Interaction of Metal Complexes with G-Quadruplex DNA. *Angew. Chem., Int. Ed.* **2010**, *49* (24), 4020−4034. (b) Liu, W.; Zhong, Y.-F.; Liu, L.-Y.; Shen, C.-T.; Zeng, W.; Wang, F.; Yang, D.; Mao, Z.-W. Solution structures of multiple G-quadruplex complexes induced by a platinum(II)-based tripod reveal dynamic binding. *Nat. Commun.* **2018**, *9* (1), 3496. (c) Reed, J. E.; Arnal, A. A.; Neidle, S.; Vilar, R. Stabilization of G-Quadruplex DNA and Inhibition of Telomerase Activity by Square-Planar Nickel(II) Complexes. *J. Am. Chem. Soc.* **2006**, *128* (18), 5992−5993. (d) Cao, Q.; Li, Y.; Freisinger, E.; Qin, P. Z.; Sigel, R. K. O.; Mao, Z.-W. G-quadruplex DNA targeted metal complexes acting as potential anticancer drugs. *Inorg. Chem. Front.* **2017**, *4* (1), 10−32. (e) Xu, C. X.; Shen, Y.; Hu, Q.; Zheng, Y. X.; Cao, Q.; Qin, P. Z.; Zhao, Y.; Ji, L. N.; Mao, Z. W. Stabilization of human telomeric G-quadruplex and inhibition of telomerase activity by propeller-shaped trinuclear Pt(II) complexes. *Chem. - Asian J.* **2014**, *9* (9), 2519−26.

(11) Chilka, P.; Desai, N.; Datta, B. Small Molecule Fluorescent Probes for G- Quadruplex Visualization as Potential Cancer Theranostic Agents. *Molecules* **2019**, *24*, 752.

(12) (a) Liu, Z.; Nalluri, S. K. M.; Stoddart, J. F. Surveying macrocyclic chemistry: from flexible crown ethers to rigid cyclophanes. *Chem. Soc. Rev.* **2017**, *46* (9), 2459−2478. (b) Radecka-Paryzek, W.; Patroniak, V.; Lisowski, J. Metal complexes of polyaza and polyoxaaza Schiff base macrocycles. *Coord. Chem. Rev.* **2005**, *249* (21), 2156−2175. (c) Patroniak, V.; Kubicki, M.; Mondry, A.; Lisowski, J.; Radecka-Paryzek, W. Pentaaza macrocyclic ytterbium-(III) complex and solvent controlled supramolecular self-assembly of its dimeric μ-η2:η2 peroxo-bridged derivatives. *Dalton Trans.* **2004**, No. 20, 3295−3304. (d) Chakrabarty, R.; Mukherjee, P. S.; Stang, P. J. Supramolecular Coordination: Self-Assembly of Finite Two- and Three-Dimensional Ensembles. *Chem. Rev.* **2011**, *111* (11), 6810−6918. (e) Matsuoka, R.; Nabeshima, T. Functional Supramolecular Architectures of Dipyrrin Complexes. *Front. Chem.* **2018**, *6*, 349.

(13) (a) Bordbar, M.; Tavoosi, F.; Yeganeh-Faal, A.; Zebarjadian, M. H. Interaction study of some macrocyclic inorganic schiff base complexes with calf thymus DNA using spectroscopic and voltammetric methods. *J. Mol. Struct.* **2018**, *1152*, 128−136. (b) Mames, I.; Rodger, A.; Kowalski, J. Tetraaza[14]macrocyclic Transition Metal Complexes as DNA Intercalators. *Eur. J. Inorg. Chem.* **2015**, *2015* (4), 630−639. (c) Liu, J.; Zhang, H.; Chen, C.; Deng, H.; Lu, T.; Ji, L. Interaction of macrocyclic copper(II) complexes with calf thymus DNA: effects of the side chains of the ligands on the DNA-binding behaviors. *Dalton Trans.* **2003**, No. 1, 114−119. (d) Kozłowski, M.; Kierzek, R.; Kubicki, M.; Radecka-

Paryzek, W. Metal-promoted synthesis, characterization, crystal structure and RNA cleavage ability of 2,6-diacetylpyridine bis(2-aminobenzoylhydrazone) lanthanide complexes. *J. Inorg. Biochem.* **2013**, *126*, 38−45. (e) Shahabadi, N.; Hakimi, M.; Morovati, T.; Fatahi, N. DNA binding affinity of a macrocyclic copper(II) complex: Spectroscopic and molecular docking studies. *Nucleosides, Nucleotides Nucleic Acids* **2017**, *36* (8), 497−510. (f) Morrow, J. R.; Buttrey, L. A.; Shelton, V. M.; Berback, K. A. Efficient catalytic cleavage of RNA by lanthanide(III) macrocyclic complexes: toward synthetic nucleases for in vivo applications. *J. Am. Chem. Soc.* **1992**, *114* (5), 1903−1905.

(14) (a) Gregoliński, J.; Kochel, A.; Lisowski, J. Lanthanide complexes of 2 + 2 meso-type macrocycle derived from trans-1,2-diaminocyclohexane and 2,6-diformylpyridine: X-ray crystal structures of La(III) and Sm(III) complexes. *Polyhedron* **2006**, *25* (14), 2745−2754. (b) Carcelli, M.; Ianelli, S.; Pelagatti, P.; Pelizzi, G.; Rogolino, D.; Solinas, C.; Tegoni, M. Synthesis and characterization of new lanthanide complexes with hexadentate hydrazonic ligands. *Inorg. Chim. Acta* **2005**, *358* (4), 903−911. (c) Arif, A. M.; Backer-Dirks, J. D. J.; Gray, C. J.; Hart, F. A.; Hursthouse, M. B. Syntheses, X-ray structures, and properties of complexes of macrocyclic hexaimines with lanthanide nitrates. *J. Chem. Soc., Dalton Trans.* **1987**, No. 7, 1665−1673.

(15) Groom, C. R.; Bruno, I. J.; Lightfoot, M. P.; Ward, S. C. The Cambridge Structural Database. *Acta Crystallogr., Sect. B: Struct. Sci., Cryst. Eng. Mater.* **2016**, *72* (2), 171−179.

(16) Dai, J.; Punchihewa, C.; Ambrus, A.; Chen, D.; Jones, R. A.; Yang, D. Structure of the intramolecular human telomeric G-quadruplex in potassium solution: a novel adenine triple formation. *Nucleic Acids Res.* **2007**, *35* (7), 2440−50.

(17) Zhai, Q.; Gao, C.; Ding, J.; Zhang, Y.; Islam, B.; Lan, W.; Hou, H.; Deng, H.; Li, J.; Hu, Z.; Mohamed, H. I.; Xu, S.; Cao, C.; Haider, S. M.; Wei, D. Selective recognition of c-MYC Pu22 G-quadruplex by a fluorescent probe. *Nucleic Acids Res.* **2019**, *47* (5), 2190−2204.

(18) Ambrus, A.; Chen, D.; Dai, J.; Bialis, T.; Jones, R. A.; Yang, D. Human telomeric sequence forms a hybrid-type intramolecular G-quadruplex structure with mixed parallel/antiparallel strands in potassium solution. *Nucleic Acids Res.* **2006**, *34* (9), 2723−2735.

(19) Dai, J.; Carver, M.; Yang, D. Polymorphism of human telomeric quadruplex structures. *Biochimie* **2008**, *90* (8), 1172−1183.

(20) Huang, F.-C.; Chang, C.-C.; Wang, J.-M.; Chang, T.-C.; Lin, J.-J. Induction of senescence in cancer cells by the G-quadruplex stabilizer, BMVC4, is independent of its telomerase inhibitory activity. *Br. J. Pharmacol.* **2012**, *167* (2), 393−406.

(21) Mendez, M. A.; Szalai, V. A. Fluorescence of unmodified oligonucleotides: A tool to probe G-quadruplex DNA structure. *Biopolymers* **2009**, *91* (10), 841−850.

(22) Lakowicz, J. R. *Principles of Fluorescence*; Springer: Boston, MA, 2006.

(23) Sarwar, T.; Rehman, S. U.; Husain, M. A.; Ishqi, H. M.; Tabish, M. Interaction of coumarin with calf thymus DNA: deciphering the mode of binding by in vitro studies. *Int. J. Biol. Macromol.* **2015**, *73*, 9−16.

(24) Mandal, P.; Sahoo, D.; Saha, S.; Chowdhury, J. Sensing of Different Human Telomeric G-Quadruplex DNA Topologies by Natural Alkaloid Allocryptopine Using Spectroscopic Techniques. *J. Phys. Chem. B* **2018**, *122* (45), 10279−10290.

(25) Chauhan, A.; Paul, R.; Debnath, M.; Bessi, I.; Mandal, S.; Schwalbe, H.; Dash, J. Synthesis of Fluorescent Binaphthyl Amines That Bind c-MYC G-Quadruplex DNA and Repress c-MYC Expression. *J. Med. Chem.* **2016**, *59* (15), 7275−7281.

(26) Ambrus, A.; Chen, D.; Dai, J.; Bialis, T.; Jones, R. A.; Yang, D. Human telomeric sequence forms a hybrid-type intramolecular G-quadruplex structure with mixed parallel/antiparallel strands in potassium solution. *Nucleic Acids Res.* **2006**, *34* (9), 2723−35.

(27) (a) Musumeci, D.; Platella, C.; Riccardi, C.; Merlino, A.; Marzo, T.; Massai, L.; Messori, L.; Montesarchio, D. A first-in-class and a fished out anticancer platinum compound: cis-$[PtCl_2(NH_3)_2]$ and cis-$[PtI_2(NH_3)_2]$ compared for their reactivity towards DNA model systems. *Dalton Trans.* **2016**, *45* (20), 8587−600. (b) Lam, E. Y. N.; Beraldi, D.; Tannahill, D.; Balasubramanian, S. G-quadruplex structures are stable and detectable in human genomic DNA. *Nat. Commun.* **2013**, *4* (1), 1796. (c) Shi, S.; Geng, X.; Zhao, J.; Yao, T.; Wang, C.; Yang, D.; Zheng, L.; Ji, L. Interaction of $[Ru(bpy)_2(dppz)]^{2+}$ with human telomeric DNA: preferential binding to G-quadruplexes over i-motif. *Biochimie* **2010**, *92* (4), 370−7.

(28) Musumeci, D.; Roviello, V.; Roviello, G. N. DNA- and RNA-binding ability of oligoDapT, a nucleobase-decorated peptide, for biomedical applications. *Int. J. Nanomed.* **2018**, *13*, 2613−2629.

https://dx.doi.org/10.1021/acs.inorgchem.0c03260
Inorg. Chem. 2021, 60, 2122−2126